On Fault-Tolerant Control of a Hovering AUV with Four Horizontal and Two Vertical Thrusters

Jin-Kyu Choi and Hayato Kondo
Tokyo University of Marine Science and Technology
2-1-6 Etchujima, Koto-ku, Tokyo 135-8533, Japan

***Abstract*-This paper discusses fault-tolerant control of a hovering AUV with four horizontal and two vertical thrusters. Three thruster fault cases are considered: the first one is when any one of the four horizontal thrusters is faulty; the second is when any two of the four horizontal thrusters are faulty; and the third is when any two of the four horizontal thrusters and any one of the two vertical thrusters are faulty. Through a series of simulations, it is shown that the AUV can track a planned path on a horizontal plane with minimally three thrusters (two are horizontal ones); however, some cases require sideways motion, cruising AUV-like motion, and oblique motion. Additionally, we briefly introduce our AUV simulator that can run hardware-in-the-loop simulation.**

I. INTRODUCTION

Autonomous underwater vehicles (AUVs) are generally self-contained and hold capabilities to take appropriate actions to deal with a variety of situations. This nature makes it possible to accomplish assigned missions, e.g., the exploration of bathymetry feature and underwater resources, in a wide area without an umbilical cable for human intervention [1].

AUVs are usually classified into two types: one is cruising AUVs [2, 3] and the other is hovering AUVs [4, 5]. Cruising AUVs typically have thrusters less than required DOFs and control surfaces for the remained DOFs. A combination of the thrusters and surfaces produces aircraft-like motion; however, it usually cannot generate hovering motion to stay at the same position for fine observation. Contrarily, hovering AUVs typically have no control surface and instead have more thrusters than required DOFs. This type of AUVs can make hovering and moving motions in various directions and hence they are widely used for inspection works that require fine motions such as port facility inspection [4] and ship hull inspection [5]. Moreover, the thruster redundancy of hovering AUVs allows to complete a given mission and to return to the support vessel, even though one or more thrusters are malfunctioned. This fault-tolerant capability reduces costs and human efforts and especially plays a crucial role in homing in case of thruster failure during explorations of underwater cave and glacier. In this paper, we discuss fault-tolerant control of a hovering AUV with six thrusters, four for horizontal motions and two for vertical motions.

Fig. 1 shows the target AUV of which four thrusters are placed horizontally for surge, sway, and yaw motions (one forward, one aft, one starboard, and one port) and two thrusters are placed vertically for heave and pitch motions (one forward and one aft). The number of the vertical thrusters is the same as the number of the required DOFs (2-DOFs, heave and pitch) and that of the horizontal thrusters is greater than the required 3-DOFs (surge, sway, and yaw). The roll motion does not be actively controlled but the vertical distance between the center of mass and the center of buoyancy stabilizes the roll motion. Generally, when the number of the thrusters is greater or equal to the number of DOFs, control inputs for controlling the DOFs exist. Yang et al. presented a fault-tolerant control method using the constrained-based method [6] and Podder et al. and Omerdic et al. presented the methods using the weighted pseudoinversion [7, 8]; however, these are all using the thruster redundancy and the case when the number of thrusters is less than required DOFs, i.e., underactuated case, has not been considered.

Fig. 1 Target hovering AUV of this study, which has been developed by the research group at Tokyo University of Marine Science and Technology, Japan. The AUV has four horizontal thrusters for surge, sway, and yaw motions and two vertical thrusters for heave and pitch motions.

In this paper, we deal with fault-tolerant control for the case when maximally three thrusters are fully malfunctioned. The following three cases are considered: (i) any one of the four horizontal thrusters is faulty (number of the horizontal thrusters=3-DOFs for horizontal motions); (ii) any two of the four horizontal thrusters are faulty (number of horizontal thrusters<3-DOFs for horizontal motions); and (iii) any two of the four horizontal thrusters and any one of the two vertical thrusters are faulty (number of the horizontal thrusters<3-DOFs for horizontal motions AND number of the vertical thrusters<2-DOFs for vertical motions). Through a series of simulations, it will be shown that: the AUV can conduct a given mission without losing hovering property when any one horizontal thruster is broken; two horizontal thrusters (the ones starboard and port, or the ones forward and aft) are able to track a given path on a horizontal plane, however the case

978-1-4244-5222-4/10/$26.00 ©2010 IEEE

using the ones forward and aft requires sideways motion; and other cases require cruising AUV-like motion and oblique motion to track a planned path.

This paper is organized as follows. Section II investigates the thruster configuration matrix of the target AUV, which maps the forces exerted by the thrusters on the resultant forces and moments applied to the AUV. We then present fault-tolerant control methods for the cases when maximally three thrusters are malfunctioned in Section III. In Section IV, a series of simulations are carried out and the results are discussed. Finally, our AUV simulator that can run hardware-in-the-loop simulation is briefly introduced in Section V.

II. THRUSTER CONFIGURATION MATRIX

The target hovering AUV of this study (Fig. 1) has six thrusters to deal with its 5-DOF motions, i.e., surge, sway, heave, pitch, and yaw. The roll motion does not be actively controlled; instead, the vertical distance between the center of mass and the center of buoyancy automatically stabilizes the roll motion. Fig. 2 shows the arrangement of thrusters and the motions to be generated by the thrusters. Four thrusters are placed horizontally for surge, sway, and yaw motions (one starboard (#1), one port (#2), one forward (#3), and one aft (#4)) and two are placed vertically for heave and pitch motions (one forward (#5) and one aft (#6)). In what follows, we investigate the thruster configuration matrix of the target AUV, which maps the thrusts exerted by the thrusters on the resultant forces and moments applied to the AUV.

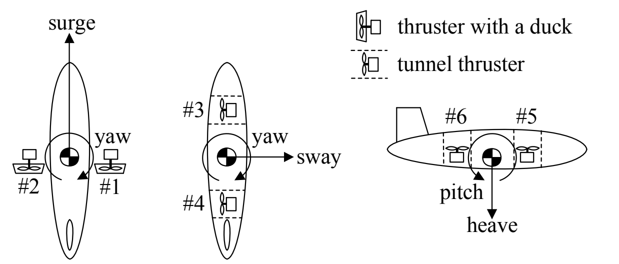

(a) horizontal motions (top view) (b) vertical motions (side view)

Fig. 2 (a) Surge, sway, and yaw motions are generated by the four horizontal thrusters (#1-#4) and (b) heave and pitch motions are by the two vertical thrusters (#5 and #6). The yaw motion can be produced by both pairs (#1, #2) and (#3, #4).

Let $\boldsymbol{\tau} \in \Re^5$ be the resultant forces and moments acting on the AUV and $\boldsymbol{T} \in \Re^6$ be the thruster forces. Then, the relationship between $\boldsymbol{\tau}$ and $\boldsymbol{T}$ is given by:

$$\boldsymbol{\tau} = B\boldsymbol{T} \tag{1}$$

where $B \in \Re^{5\times6}$ is *the thruster configuration matrix* and its elements are determined by the geometrical configuration of thrusters. Eq. (1) can be rewritten into:

$$\begin{pmatrix} \boldsymbol{\tau}_H \\ \boldsymbol{\tau}_V \end{pmatrix} = \begin{pmatrix} B_H & O_{3\times2} \\ O_{2\times4} & B_V \end{pmatrix} \begin{pmatrix} \boldsymbol{T}_H \\ \boldsymbol{T}_V \end{pmatrix} \tag{2}$$

where, $\boldsymbol{\tau}_H = (F_x, F_y, M_z)^T \in \Re^3$,

$\boldsymbol{\tau}_V = (F_z, M_y)^T \in \Re^2$,

$\boldsymbol{T}_H = (T_1, T_2, T_3, T_4)^T \in \Re^4$,

$\boldsymbol{T}_V = (T_5, T_6)^T \in \Re^2$,

F_x, F_y, and F_z are the resultant forces acting along the x-, y-, and z-axis of the body frame attached at the AUV, respectively, M_y and M_z are the resultant moments around the y- and z-axis, respectively, and T_i is the force exerted by the #i thruster. Additionally, $B_H \in \Re^{3\times4}$ and $B_V \in \Re^{2\times2}$ are the thruster configuration matrices associated with the horizontal and vertical thrusters, respectively, and their elements are:

$$B_H = \begin{pmatrix} 1 & 1 & 0 & 0 \\ 0 & 0 & 1 & 1 \\ -a & a & b & -b \end{pmatrix} \tag{3}$$

$$B_V = \begin{pmatrix} 1 & 1 \\ -c & c \end{pmatrix} \tag{4}$$

where, a is the horizontal distance from the center of the AUV to the axis of the #1 or #2 thruster, b to the #3 or #4 thruster, and c to the #5 or #6 thruster.

From Eq. (2), it is shown that $\boldsymbol{\tau}_H$ is free of the influence of $\boldsymbol{T}_V$ and $\boldsymbol{\tau}_V$ does so about $\boldsymbol{T}_H$. Hence, Eq. (2) can be divided into the following two parts (horizontal and vertical parts, respectively):

$$\boldsymbol{\tau}_H = B_H \boldsymbol{T}_H \tag{5}$$

$$\boldsymbol{\tau}_V = B_V \boldsymbol{T}_V . \tag{6}$$

Here, in order to exert resultant forces and moments for producing desired horizontal motions, Eq. (5) should satisfy:

$$\text{rank}(B_H) \le \dim(\boldsymbol{T}_H) . \tag{7}$$

Likewise, for vertical motions, Eq. (6) should hold:

$$\text{rank}(B_V) \le \dim(\boldsymbol{T}_V) . \tag{8}$$

As for the target AUV, these two conditions are satisfied since

$$\text{rank}(B_H)=3<\dim(\boldsymbol{T}_H)=4 \text{ AND } \text{rank}(B_V)=\dim(\boldsymbol{T}_V)=2. \tag{9}$$

Thus, the AUV is able to generate desired horizontal and vertical motions by its six thrusters. From Eqs. (3) and (9), it is clear that the condition in Eq. (7) is satisfied even if one horizontal thruster is completely broken. This implies that the target AUV intrinsically has a fault-tolerant capability for horizontal motions.

III. FAULT-TOLERANT CONTROL

It is assumed that: a faulty thruster(s) has been detected; the detected faulty thruster is totally malfunctioned; and external disturbances, e.g., sea current, do not be considered. The following thruster faulty situations are considered:

(i) $\text{rank}(B_H)<\dim(\boldsymbol{T}_H)$ AND $\text{rank}(B_V)=\dim(\boldsymbol{T}_V)$: when there is no faulty thruster.

(ii) $\text{rank}(B_H)=\dim(\boldsymbol{T}_H)$ AND $\text{rank}(B_V)=\dim(\boldsymbol{T}_V)$: when one horizontal thruster is faulty.

(iii) $\text{rank}(B_H)>\dim(\boldsymbol{T}_H)$ AND $\text{rank}(B_V)=\dim(\boldsymbol{T}_V)$: when two horizontal thrusters are faulty.

(iv) $\text{rank}(B_H)>\dim(\boldsymbol{T}_H)$ AND $\text{rank}(B_V)>\dim(\boldsymbol{T}_V)$: when two horizontal thrusters and one vertical thruster are faulty, i.e., totally three thrusters are faulty.

Here, $\dim(\boldsymbol{T}_H)$ and $\dim(\boldsymbol{T}_V)$ do not include the faulty thruster(s). Path-tracking control for these cases will be discussed below.

A. When rank(B_H)<dim($\boldsymbol{T}_H$) AND rank(B_V)=dim($\boldsymbol{T}_V$)

This condition is met when no thruster is faulty. In this case, the vertical thruster forces for desired vertical motions can be obtained by simple inversion of B_V , but the horizontal ones need to be obtained using the pseudoinversion of B_H. Specifically, $\boldsymbol{T}_H$ is given as:

$$\boldsymbol{T}_H = W_H^{-1} B_H^T (B_H W_H^{-1} B_H^T)^{-1} \boldsymbol{\tau}_H \tag{10}$$

where, W_H=diag(w_1, w_2, w_3, w_4) is a weighting matrix, w_i>0, $W_H=I_{4\times4}$ for this case, and $I_{i\times j}$ is a $i\times j$ identity matrix.

Additionally, $\boldsymbol{\tau}_H$ and $\boldsymbol{\tau}_V$ are obtained as below. For convenience, let F and M be the resultant force and moment applied to the AUV, respectively. Then, F for surge, sway, and heave motions is given by:

$$F = k_v (v_r - v) \tag{11}$$

where, $v_r=k_p\|\boldsymbol{p}_r-\boldsymbol{p}\|$, $v_r=v_{max}$ if $v_r>v_{max}$, $v_r=-v_{max}$ if $v_r<-v_{max}$, v_r is a desired translational velocity, v is a current translational velocity, $\boldsymbol{p}_r$ is the goal position, $\boldsymbol{p}$ is a current position, and k_v>0 and k_p>0 are control gains. In a similar way, for pitch and yaw controls:

$$M = k_\omega (\omega_r - \omega) \tag{12}$$

where, $\omega_r=k_\theta(\theta_r-\theta)$, $\omega_r=\omega_{max}$ if $\omega_r>\omega_{max}$, $\omega_r=-\omega_{max}$ if $\omega_r<-\omega_{max}$, ω_r is a desired rotational velocity, ω is a current rotational velocity, θ_r is the goal rotational angle, θ is a current rotational angle, and k_ω>0 and k_θ>0 are control gains. In upper two controls, the control gains k_p and k_θ determine the rate of change of acceleration and deceleration, and if k_v and k_ω have large values, $v\approx v_r$ and $\omega\approx\omega_r$.

B. When rank(B_H)=dim($\boldsymbol{T}_H$) AND rank(B_V)=dim($\boldsymbol{T}_V$)

Although one horizontal thruster is malfunctioned, the condition in Eq. (7) is still satisfied. Hence, the horizontal thruster forces for desired horizontal motions can be determined. As the normal situation (the case of Subsection *A*), the vertical thruster forces are given by simple inversion of B_V and the horizontal ones are by the pseudoinversion of B_H (Eq. (10)). In this case, giving an infinite value to the corresponding weight w_i, the faulty thruster does not work in Eq. (10). $\boldsymbol{\tau}_H$ and $\boldsymbol{\tau}_V$ are obtained by Eqs. (11) and (12).

C. When rank(B_H)>dim($\boldsymbol{T}_H$) AND rank(B_V)=dim($\boldsymbol{T}_V$)

The vertical motions can be sufficiently controlled like former two cases, but the horizontal motions are different because two faulty thrusters result in rank(B_H)>dim($\boldsymbol{T}_H$), this is contrary to the condition in Eq. (7).

1) When the #3 and #4 thrusters are faulty

When the #3 and #4 thrusters are inactive, Eq. (5) can be rewritten into the following reduced form:

$$\underbrace{\begin{pmatrix} F_x \\ M_z \end{pmatrix}}_{\boldsymbol{\tau}'_H} = \underbrace{\begin{pmatrix} 1 & 1 \\ -a & a \end{pmatrix}}_{B'_H} \underbrace{\begin{pmatrix} T_1 \\ T_2 \end{pmatrix}}_{\boldsymbol{T}_H} \tag{13}$$

and in this case,

$$\text{rank}(B'_H) = \dim(\boldsymbol{T}_H) \ . \tag{14}$$

From Eq. (14) and the fact that $F_x\neq0$, M_Z=0 when $T_1=T_2$ and F_x=0, $M_Z\neq0$ when $T_1=-T_2$, it is clear that the remained #1 and #2 thrusters can control surge and yaw motions independently. Usually, hovering AUVs track a planned path given on a horizontal plane by using surge and yaw motions and hence the remained two thrusters can accomplish a given mission. Setting the weights related to the two faulty thrusters as infinite values, the forces exerted by the #1 and #2 thrusters can be obtained by Eq. (10); however, it is efficient to use Eq. (13) for reducing the computational time. Eqs. (11) and (12) yield $\boldsymbol{\tau}_H$ and $\boldsymbol{\tau}_V$ and Fig. 3(a) shows an example of tracking a planned path using only surge and yaw motions.

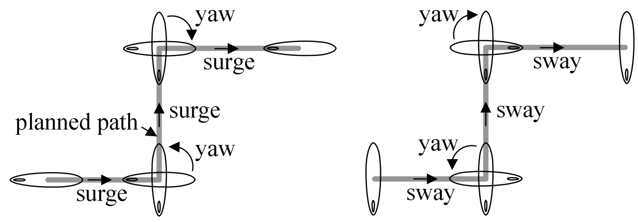

Fig. 3 Tracking a planned path on a horizontal plane. (a) Using surge and yaw motions. (b) Using sway and yaw motions.

2) When the #1 and #2 thrusters are faulty

Similar to the case when the #3 and #4 thrusters are faulty, Eq. (5) can be rewritten into:

$$\underbrace{\begin{pmatrix} F_y \\ M_z \end{pmatrix}}_{\boldsymbol{\tau}'_H} = \underbrace{\begin{pmatrix} 1 & 1 \\ b & -b \end{pmatrix}}_{B'_H} \underbrace{\begin{pmatrix} T_3 \\ T_4 \end{pmatrix}}_{\boldsymbol{T}_H} \tag{15}$$

and for this case:

$$\text{rank}(B'_H) = \dim(\boldsymbol{T}_H) \ . \tag{16}$$

From Eq. (16) and the fact that $F_y\neq0$, M_Z=0 when $T_3=T_4$ and F_y=0, $M_Z\neq0$ when $T_3=-T_4$, the sway and yaw motions can be independently controlled. As shown in Fig. 3(b), sway and yaw motions also can complete a given mission; however, much more thrusts are necessary due to larger hydrodynamic damping than the case of Fig. 3(a). Surely, Eq. (10) or Eq. (15) also supplies the horizontal thruster forces and Eqs. (11) and (12) give $\boldsymbol{\tau}_H$ and $\boldsymbol{\tau}_V$.

3) When the thruster pair (#1, #3) or (#1, #4) or (#2, #3) or (#2, #4) is faulty

For these cases,

$$\underbrace{\begin{pmatrix} F_x \\ F_y \\ M_z \end{pmatrix}}_{\boldsymbol{\tau}'_H} = \underbrace{\begin{pmatrix} 1 & 0 \\ 0 & 1 \\ \beta & \gamma \end{pmatrix}}_{B'_H} \underbrace{\begin{pmatrix} T_i \\ T_j \end{pmatrix}}_{\boldsymbol{T}_H} \tag{17}$$

$$\text{rank}(B'_H) > \dim(\boldsymbol{T}_H) \tag{18}$$

where, $\beta=-a$ when i=1, $\beta=a$ when i=2, $\gamma=b$ when j=3, and $\gamma=-b$ when j=4. Unlike the cases of Eqs. (13) and (15), the thruster forces for desired motions cannot be determined in this case because the number of thrusters is less than the number of the resultant forces and moments as shown in Eq. (18).

In order to solve this control problem, we introduce F_{ij} as shown in Fig. 4(a), which passes through the center of gravity so as not to exert a moment producing the yaw motion. Then, controlling F_{ij} (forward velocity) and M_z (rotational velocity) can make the path-tracking possible; however, the navigation style is not of hovering AUVs but of cruising AUVs. Fig. 4(b) shows an example of path tracking when T_2 and T_4 are broken, i.e., T_1 and T_3 are active.

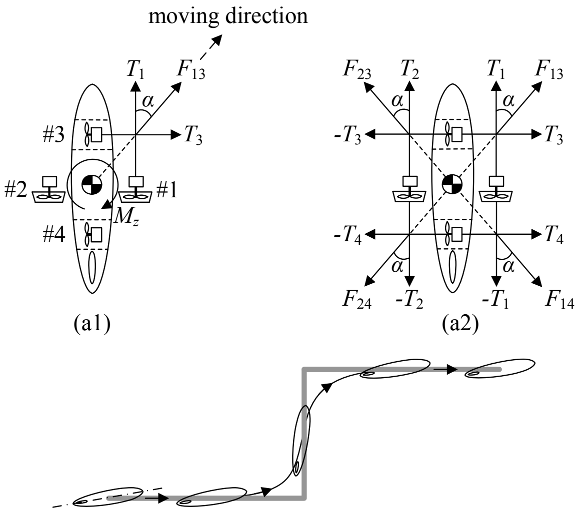

(b) when T_1 and T_3 are active

Fig. 4 (a) F_{ij} exerted by T_i and T_j enables the AUV to move without exerting a moment that produces the yaw motion. (b) Path tracking by controlling both F_{13} and M_z (a moment producing the yaw motion for heading control).

Specifically, the thrsuter forces T_i and T_j can be obtained from the relationship:

$$\begin{pmatrix} F_{ij} \\ M_z \end{pmatrix} = \begin{pmatrix} \sigma_1 \cos\alpha & \sigma_2 \sin\alpha \\ -\sigma_2 a & \sigma_1 b \end{pmatrix} \begin{pmatrix} T_i \\ T_j \end{pmatrix} \quad (19)$$

where, $\alpha=\tan^{-1}(a/b)$, $\sigma_1=\sigma_2=1$ for F_{13}, $\sigma_1=-1$ and $\sigma_2=1$ for F_{14}, $\sigma_1=1$ and $\sigma_2=-1$ for F_{23}, and $\sigma_1=\sigma_2=-1$ for F_{24}. Additionally, F_{ij} and M_z are obtained by Eqs. (11) and (12); however, ω_r is given by:

$$\omega_r = -k_y \eta_y + k_\psi \eta_\psi \quad (20)$$

where, η_y is the y-position of the $O_pX_pY_p$-frame as shown in Fig. 5, $\eta_y=\psi_p-(\psi+\varepsilon)$, $\varepsilon=\alpha$ for F_{13}, $\varepsilon=\pi-\alpha$ for F_{14}, $\varepsilon=\pi+\alpha$ for F_{24}, $\varepsilon=-\alpha$ for F_{23}, and $k_y>0$ and $k_\psi>0$ are control gains. If $v\approx v_r$ and $\omega\approx\omega_r$, the AUV will be located on the X_p-axis on which a straight-line path is given, i.e., the path-tracking control will be achieved.

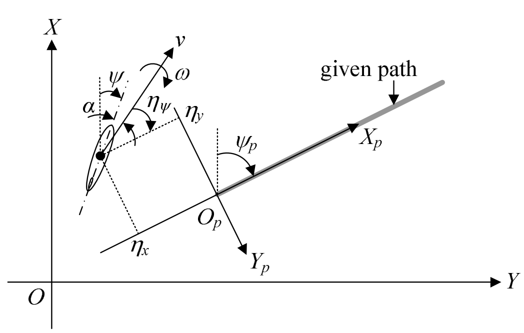

Fig. 5 Path-tracking control on a horizontal plane when the #2 and #4 thrusters are faulty (T_1 and T_3 are active).

D. When rank(B_H)>dim($\boldsymbol{T}_H$) AND rank(B_V)>dim($\boldsymbol{T}_V$)

There are two cases to be discussed: one is the case when neutral buoyancy is applied to the AUV and the other is when a slight amount of positive buoyancy is applied. First, when neutral buoyancy is applied, the depth (or altitude) control can be achieved using only one vertical thruster, because the moment balance between the one exerted by the single vertical thruster and the one by the distance between the gravity center and the buoyancy center maintains the pitch angle a constant value during ascending or descending as shown in Fig. 6; however, if the AUV reaches the goal depth and the thrust of the single vertical thruster becomes zero, the pitch angle automatically grows to zero by the gravitational and buoyant forces. Hence, the control methods presented in Subsection *C* can be used for this case.

Next, when a slight amount of positive buoyancy is applied, the pitch angle cannot be zero even if the AUV reaches the goal depth since the single vertical thruster should continually exert a force to maintain the goal depth due to the positive buoyancy. However, if the buoyancy force is small (this is usual case), the pitch angle (θ_e in Fig. 6) produced by the moment balance is also small. Consequently, the fault-tolerant control methods in Subsection *C* can be adopted for this case like the former case. Additionally, in upper two cases, the AUV descends and ascends obliquely.

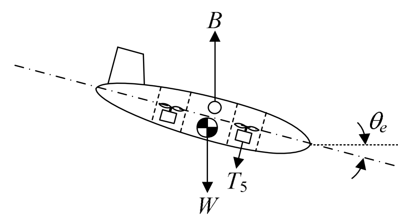

Fig. 6 The moment exerted by T_5 is in balance with the moment exerted by the gravitational force (W) and the buoyant force (B) during descending, and this produces non-zero pitch angle (θ_e).

IV. Simulation

In order to verify the effectiveness of the presented fault-tolerant control methods, simulations were carried out. The following three examples were selected: (i) when the #1 and #2 thrusters are malfunctioned; (ii) when the #2 and #3 thrusters are malfunctioned; and (iii) when the #3, #4, and #6 thrusters are malfunctioned. The parameter values used for the simulations are as follows: m=390 kg is the mass, I_x=26.34 kgm^2, I_y=305.67 kgm^2, and I_z=305.67 kgm^2 are the moments of inertia, $X_{\dot{u}}$ =-49.12, $Y_{\dot{v}}$ =-311.52, $Z_{\dot{w}}$ =-311.52, $K_{\dot{p}}$ =0, $M_{\dot{q}}$ =-87.63, and $N_{\dot{r}}$ =-87.63 are the added mass derivatives, X_u=-20, Y_v=-200, Z_w=-200, K_p=-10, M_q=-200, and N_r=-200 are the coefficients of the linear skin friction, X_{uu}=-30, Y_{vv}=-300, Z_{ww}=-300, K_{pp}=-10, M_{qq}=-300, and N_{rr}=-300 are the coefficients of the quadratic drag (refer to [9]), (0, 0, 0.15) m is the center of mass, (0, 0, -0.15) m is the center of buoyancy, a=0.47 m, b=0.8 m, c=0.63 m, and neutral buoyancy is considered for the examples (i) and (ii) and a buoyant force of 10 N is considered for the example (iii). Note that some of these parameter values are different to those of the target hovering AUV (Fig. 1) because the tank tests for evaluating them have not been carried out.

Additionally, for all the simulations, the maximum value of the thrusters' force is ±100 N, k_v=k_ω=1000, k_p=k_θ=0.5, and the given mission is to track the straight lines connecting five waypoints at the depth of 8 m. Since this paper assumes that the faulty thruster has been detected, the AUV starts the mission without the faulty thruster(s).

First, the simulations when the #1 and #2 thrusters are faulty were conducted. As shown in (a) in Fig. 7, it is clear that the AUV is able to track the lines on a horizontal plane with the #3 and #4 thrusters although sideways motions are required. The position errors during turning to the next waypoint are thought to be due to the remained inertia force resulted by the sideways (sway) motion. Fig. 8(a) shows the forces exerted by the #3 and #4 thrusters (T_3 and T_4).

Next, the simulation results when the #2 and #4 thrusters are broken (T_1, T_3, T_5, and T_6 are active) are shown in (b) in Fig. 7 and Fig. 8(b). As seen in the figure, the AUV tracks the straight lines like cruising AUVs with non-zero yaw angle. Although position errors are seen near the waypoint, the line-tracking performance at the area between two waypoints is acceptable.

Finally, the simulation results when the #3, #4, and #6 thrusters are malfunctioned, i.e., T_1, T_2, and T_5 are active, are presented in (c) in Fig. 7 and Fig. 8(c). Better performance than upper two cases is observed and it is known that even if only three thrusters are active, the path-tracking in a 3-D space can be achieved by virtue of the gravitational and buoyant forces; however, T_5 should be exerted continually in order to maintain the goal depth and the AUV needs to obliquely descend and ascend. The pitch angle during tracking the straight-line path is approximately -0.57° (the buoyant force of 10 N is applied to the AUV).

Additionally, it is observed from the simulation results that the navigation time of the case when the AUV moves like cruising AUVs is most brief and the case when moving with sideways motion takes the longest time. The reason of the former is that the cruising AUV-like navigation does not produce a rotational motion at the same position and does not necessarily pass through the waypoints (but pass through the straight-line path). Also, the larger hydrodynamic damping during doing the sideways motion is considered to be the cause of the latter. From the fact that the navigation time is proportional to energy consumption, the cruising AUV-like motion is considered to be effective when the battery is weakening.

V. Integrated AUV Simulator

We have been developing an integrated AUV simulator that can run hardware-in-the-loop simulation as well as usual simulation. In addition, a functional capability to carry out the analysis, visualization, and making a database of obtained data using GIS (Geographic Information System) is planned to be integrated into the simulator. The simulations in Section IV were conducted with this simulator.

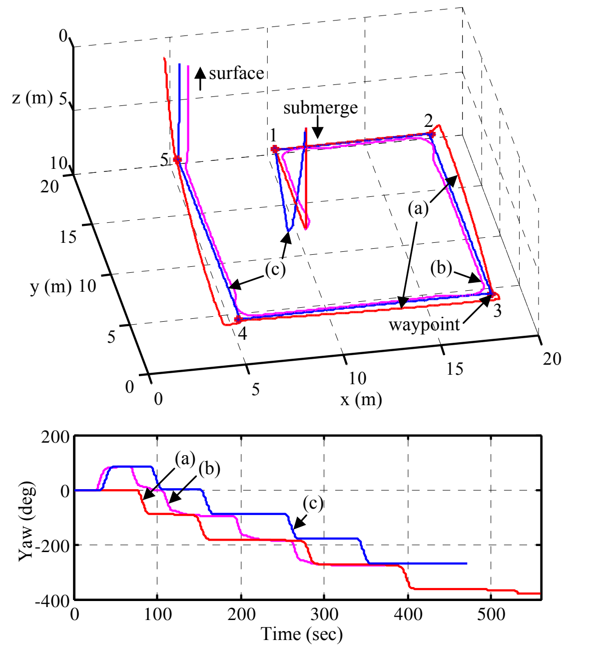

Fig. 7 Simulation results: position and the yaw angle. (a) When the #1 and #2 thrusters are malfunctioned. (b) When the #2 and #4 thrusters are malfunctioned. (c) When the #3, #4, and #6 thrusters are malfunctioned.

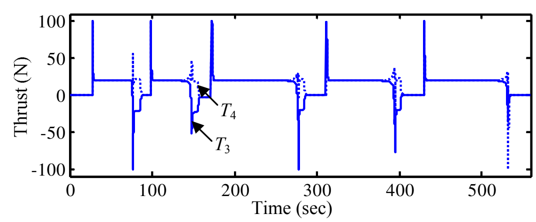

(a) when the #1 and #2 thrusters are malfunctioned

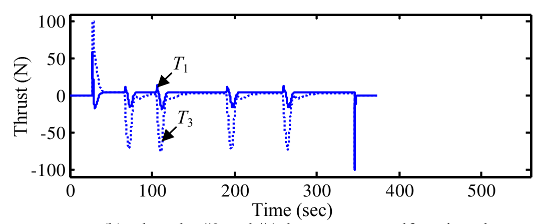

(b) when the #2 and #4 thrusters are malfunctioned

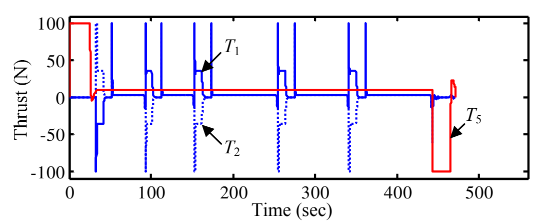

(c) when the #3, #4, and #6 thrusters are malfunctioned

Fig. 8 Simulation results: the forces exerted by the active thrusters.

Fig. 9 shows the configuration of the integrated AUV simulator. Using GUI (Graphical User Interface) shown in Fig. 10, the user can set the simulation conditions and can monitor

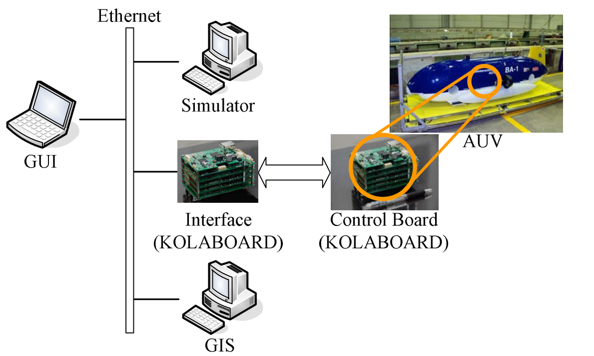

Fig. 9 Configuration of the integrated AUV simulator ("KOLABOARD" [10] is a customized control board, which was embedded in the target AUV).

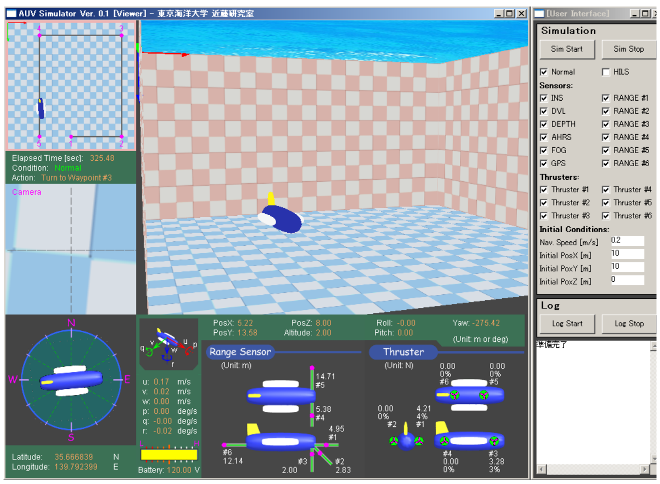
Fig. 10 GUI.

the simulation process with numerical display and 2-D and 3-D animations. Simulator shown in Fig. 9 plays a role to compute the dynamic equations of motion of the AUV together with the math models of thrusters, sensors, underwater environments, and batteries. At testing site, using one PC that has both functions of GUI and Simulator is likely to be useful.

For the hardware-in-the-loop simulation, a control board named as KOLABOARD (Kondo laboratory control board) that is identical to that embedded in the target AUV is used as an interface between the control board of the AUV and other components. The KOLABOARD is small-sized (see Fig. 9) and customized for autonomous mobile robots. It consists of four boards: main, power and peripherals board; multi-IO board; FPGA board; and GPS, wireless, LAN and A-net board. For more detailed specs, visit the website [10]. Usually, in order to run the hardware-in-the-loop simulation, a relatively large-scaled device (interface) is required to convert the physical signals from the control board of the AUV into the data needed to other components, and vice versa. Hence, using KOLABOARD can make the overall size of the simulator small. The components of the simulator communicate with each other using TCP/IP.

VI. Conclusion

This paper has presented fault-tolerant control methods for a hovering AUV with four horizontal and two vertical thrusters. The following three thruster fault cases were considered: the first one is when any one of the four horizontal thrusters is faulty; the second is when any two of the four horizontal thrusters are faulty; and the third is when any two of the four horizontal thrusters and any one of the two vertical thrusters are faulty (totally three thrusters are faulty). It was shown through simulations that: the AUV can accomplish a given mission without losing hovering property when any one horizontal thruster is malfunctioned; two horizontal thrusters (the ones starboard and port, or the ones forward and aft) are able to track a given path on a horizontal plane without losing hovering motions, however the case using the ones forward and aft requires sideways motions; and other cases require cruising AUV-like motion and oblique motion. Finally, our AUV simulator that can run hardware-in-the-loop simulation was introduced. Our future work will involve carrying out the systematization of the presented control methods and the verification of their effectiveness through experiments using the target AUV.

References

[1] T. Ura, "Autonomous Underwater Vehicle," *Journal of the Robotics Society of Japan*, Vol. 18, No. 7, pp. 933-936, 2000 (in Japanese).

[2] K. Asakawa, J. Kojima, Y. Kato, S. Matsumoto, N. Kato, T. Asai and T. Iso, "Design Concept and Experimental Results of the Autonomous Underwater Vehicle AQUA EXPLORER 2 for the Inspection of Underwater Cables," *Advanced Robotics*, Vol. 16, No. 1, pp. 27-42, 2002.

[3] T. Aoki, T. Hyakudome, T. Nakamura, K. Tamura, H. Ochi, T. Murashima, S. Tsukioka, H. Nakajoh, T. Ida, K. Akazawa and K. Hashimoto, "Deep and Long Range AUV "URASHIMA"," *Proc. the Eleventh International Offshore and Polar Engineering Conference*, pp. 314-320, 2001.

[4] H. Kondo and T. Ura, "Navigation of an AUV for Investigation of Underwater Structures," *Control Engineering Practice*, Vol. 12, pp. 1551-1559, 2004.

[5] J. Vaganay, M. Elkins, D. Esposito, W. O'Halloran, F. Hover and M. Kokko, "Ship Hull Inspection with the HAUV: US Navy and NATO Demonstration Results," *Proc. IEEE/MTS Oceans 2006*, 2006.

[6] K. C. H. Yang, J. Yuh and S. K. Choi, "Fault-tolerant System Design of an Autonomous Underwater Vehicle-ODIN: an Experimental Study," *International Journal of Systems Science*, Vol. 30, No. 9, pp. 1011-1019, 1999.

[7] T. K. Podder, G. Antonelli and N. Sarkar, "Fault Tolerant Control of an Autonomous Underwater Vehicle Under Thruster Redundancy: Simulations and Experiments," *Proc. IEEE Int. Conf. on Robotics and Automation*, pp. 1251-1256, 2000.

[8] E. Omerdic and G. Roberts, "Thruster Fault Diagnosis and Accommodation for Open-frame Underwater Vehicles," *Control Engineering Practice*, Vol. 12, pp. 1575-1598, 2004.

[9] T. I. Fossen, Marine Control Systems: Guidance, Navigation and Control of Ships, Rigs and Underwater Vehicles, *Marine Cybernetics AS*, 2002.

[10] http://resource.renesas.com/lib/jpn/superh/forum/archive/08/kolaboard_kaiyodai.pdf